Research Square

Preprints are preliminary reports that have not undergone peer review. They should not be considered conclusive, used to inform clinical practice, or referenced by the media as validated information.

A Halophilic Arsenite-Oxidizing Bacterium from the Lut Desert: Oceanobacillus picturae strain LW102 as a Promising Candidate for Arsenic Bioremediation

Nazanin Tavoosi
Islamic Azad University
Atefeh Safarpour
University of Tehran
Abbas Akhavan Sepahi
Islamic Azad University
Ram Karan
University of Delhi
Mohammad Ali Amoozegar
amoozegar@ut.ac.ir

University of Tehran

Research Article

Keywords: Halophile, Lut desert, Arsenite oxidation, Bioremediation, Bioremoval

Posted Date: October 16th, 2026

DOI: https://doi.org/10.21203/rs.3.rs-11128351/v1

License: This work is licensed under a Creative Commons Attribution 4.0 International License. Read Full License

Additional Declarations: No competing interests reported.

Abstract

Arsenic contamination in hypersaline environments is an acute ecological and public health issue that requires efficient bioremediation. Here, we present the isolation and characterization of a halophilic arsenite-oxidizing bacterium, *Oceanobacillus picturae* strain LW102, from the Lut Desert, Iran. The strain showed superb tolerance to arsenic oxyanions and other heavy metals, which was promising for its application in the bioremediation of salt and arsenic-polluted ecosystems.

Minimum inhibitory concentration (MIC) tests confirmed high resistance with MIC values of 800 mM for arsenate As^{5+}, 30 mM for arsenite As^{3+}, 1200 mM for selenite Se^{4+}, and 8 mM for cadmium Cd^{2+}. Under extreme salinity conditions (7.5% NaCl), *O. picturae* strain LW102 eliminated 80% of the arsenite in the culture solution. Arsenite removal and oxidation were assayed by Silver Diethyldithiocarbamate (SDDC) assay. Fourier Transform Infrared (FTIR) spectrometry proved the occurrence of strong interactions among arsenite and functional groups over the bacterial cell surface. Scanning Electron Microscopy with Energy Dispersive X-ray Spectroscopy (SEM-EDS) and Transmission Electron Microscopy (TEM) examination demonstrated intracellular electron-dense depositions typical for arsenic inclusion, with no significant surface morphology alterations.

The impressive heavy metal tolerance and arsenite removal capacity exhibited by *O. picturae* strain LW102, especially under hypersaline conditions, render this strain a potential arsenic bioremediation agent. Additional research on the genetic and metabolic pathways responsible for these capabilities will be needed to improve its application in environmental biotechnology.

Introduction

Arsenic (As), a toxic metalloid whose concentration is rising due to anthropogenic activities and natural processes, is linked to various cancers and severe health issues, including chronic respiratory disorders, cardiovascular problems, and reproductive complications (Patel et al. 2023; Soto et al. 2026). Arsenic exists in four oxidation states, with As^{3+} and As^{5+} being the most prevalent in the environment; As^{3+} is significantly more toxic due to its high affinity for thiol groups in proteins, leading to functional disruption, while As^{5+} is less toxic and more readily excreted (Yadav et al. 2024; Yang et al. 2022).

Conventional arsenic removal techniques, such as ion exchange and reverse osmosis, generate significant arsenic-laden sludge and incur high operational costs, making them less eco-friendly. In contrast, bioremediation using microorganisms presents a sustainable and cost-effective alternative for arsenic decontamination (Sher et al. 2021a). Microorganisms employ various mechanisms to detoxify arsenic, including oxidation-reduction processes that convert toxic arsenite (As^{3+}) to less toxic arsenate (As^{5+}). This microbial oxidation of arsenite is more efficient than traditional methods, which rely on time-consuming natural reactions or hazardous chemical agents. Focusing on halophilic arsenic-oxidizing microorganisms could enhance bioremediation strategies in saline environments, offering a promising solution for arsenic contamination (Rodriguez-Castrejon et al. 2022; Bhowmik et al. 2025; Jebelli et al. 2018; Dey et al. 2016).

Arsenite oxidation ability has been reported in different bacterial strains, including *Bacillus flexus* strain SSAI1, *Pseudomonas chengduensis* strain As-11, *Bacillus flexus* strain As-12, *Klebsiella pneumoniae* strain SSSW7, *Lysinibacillus boronitolerans* strain P2IIIb, and *Pseudomonas* sp. strain SM11 (Jebelli et al. 2018; Mujawar et al. 2019, 2021; Aguilar et al. 2020; He et al. 2023). However, many arsenic-resistant bacteria have been reported, only a limited number of studies have focused on the bioremediation potential of halophilic or halotolerant bacteria under high-salinity conditions (Voica et al. 2016). Halophilic and halotolerant bacteria can grow in saline environments and maintain their osmotic balance with the external medium. Therefore, they are promising candidates for the bioremediation of polluted saline regions (Baati et al. 2020).

The Lut Desert, located in the southeast of Iran, is one of the largest salt deserts in the world. It is also known as one of Earth's driest and hottest places. The desert covers one-tenth of Iran's area and spans several provinces, including South Khorasan, Sistan Baluchestan, and Kerman. Numerous gold, copper, iron, zinc, and coal mines and associated activities in the Lut Desert regions, as well as natural incidents like volcanic and seismic activities, lead to heavy metal pollution in the surrounding environments. Considering that the Lut Desert has a complex topography with strong seasonal winds, the toxic metals can be transported into the desert and nearby urban areas and cause serious health issues. In addition, high concentrations of toxic heavy metals such as mercury and arsenic have been reported in the eastern and central parts of Iran (Kalankesh et al. 2022; Shirsalimian et al. 2022).

In this study, we aimed to isolate and characterize arsenite-tolerant halophilic or halotolerant bacteria from the soil of the Lut Desert. Then, the most arsenite-tolerant strain was selected for further investigation, where we evaluated the effects of various physicochemical parameters on its growth in both the absence and presence of arsenite. Additionally, we explored the potential for arsenite oxidation and removal using the Silver Diethyldithiocarbamate (SDDC) method. For a better understanding of the mechanisms of arsenite resistance, we employed advanced techniques such as Fourier Transform Infrared (FTIR) spectroscopy, Scanning Electron Microscopy with Energy Dispersive X-ray Spectroscopy (SEM-EDS), and Transmission Electron Microscopy (TEM) under optimal growth conditions.

Materials and methods

Study area selection and sample collection

The soil and water of the Lut Desert in the east and southeast of Iran are polluted with various heavy metals due to numerous mining activities and its arid climate (Kalankesh et al. 2022). Soil samples were collected aseptically from four different sites of the central Lut Desert area: W7 (30°, 50′, 00.10″N 61°, 40′, 00.06″E), W8 (29°, 48′, 59″N 59°, 04′, 04″E), W9 (30°, 50′, 30.62″N 61°, 09′, 32.83″E), and W10 (29°, 48′, 46.2″N, 59°, 04′, 07″E) according to Fig. S1. The Lut Desert, particularly the central region, is known for its extremely arid climate, excessive summer heat, and annual precipitation of less than 30 mm (Lyons et al. 2020). The soil samples were collected and stored in sterile polythene bags before being transported to the laboratory for further processing. Upon arrival, several physicochemical parameters of the samples were evaluated, including temperature, pH, salinity, electrical conductivity, color, and texture. The pH of all samples was evaluated under controlled conditions using a calibrated pH meter (Mettler Toledo, Singapore). Salinity was determined using a conductivity meter (Mettler Toledo, Singapore). Electrical conductivity was assessed in the same soil-water suspension used for pH analysis. The color of the soil samples was visually classified according to standard color charts. Soil texture analysis was conducted using the hydrometer method, allowing the determination of sand, silt, and clay fractions.

Isolation of halotolerant/halophilic arsenite-tolerant bacteria

The enrichment and isolation of halotolerant/halophilic bacteria was done according to Amoozegar et al. (Amoozegar et al. 2005) with some modifications. Collected soil samples (1g) were added to Erlenmeyer flasks containing 20 mL of MH-10 (Moderate Halophilic broth with a final total salts concentration of 10% (w/v) (g L^{-1})): (NaCl, 80; $MgCl_2.6H_20$, 7; $MgSO_4.7H_2O$, 8; $CaCl_2$, 0.36; KCl, 2; $NaHCO_3$, 0.06; NaBr, 0.026; yeast extract (YE), 1; peptone from meat, 5) (Schneegurt et al. 2012). Then, the flasks were incubated under orbital shaking at 150 rpm and 37 °C for 2 days. After incubation, enrichment cultures that showed turbidity were subcultured on MH-10 agar and incubated at 37 °C for 2 days. Morphologically distinct bacterial colonies were selected and streaked on the same solid medium at least three times to obtain pure cultures. Pure halotolerant/halophilic bacterial colonies were cultured on the SW-10 (Sea Water medium containing 10% (w/v) total salts concentration (g L^{-1})): (NaCl, 81; $MgCl_2$, 7; $MgSO_4$, 9.6; $CaCl_2$, 0.36; KCl, 2; $NaHCO_3$, 0.06;

NaBr, 0.026, yeast extract (YE), 1; agar, 20) and amended with 5 mM of sodium arsenite (Nieto et al. 1989). Then, arsenite-tolerant bacteria were subjected to further investigations.

Determination of the minimum inhibitory concentration (MIC)

The minimum inhibitory concentration (MIC) of the arsenite-tolerant halotolerant/halophilic bacteria towards arsenic oxyanions and seven different toxic heavy metals/oxyanions was determined using an agar dilution method. For this purpose, SW-10 agar media supplemented with incremental concentrations of both arsenic oxyanions (As^{5+} (1-1600 mM) and As^{3+} (1–40 mM)) and seven toxic heavy metals/oxyanions (Pb^{2+} (1–40 mM), Cd^{2+} (1–14 mM), Zn^{2+} (1–4 mM), Cu^{2+} (1–8 mM), Cr^{6+}(1–10 mM), Se^{4+} (1-1400 mM), and Hg^{2+} (0.5–1.5 mM)) were prepared separately. Bacterial isolates were inoculated on SW-10 agar plates, and after 48 h of incubation at 37 °C, bacterial colonies' formation on agar plates was checked. The bacterial isolate that showed the highest MIC value for arsenite on SW-10 agar was also subjected to MIC evaluation in SW-10 broth. Hence, SW-10 broth medium with increasing concentrations of arsenite was inoculated with the selected isolate and incubated at 37 °C, 150 rpm for 48 h. The growth was monitored by measuring absorbance at 600 nm. In addition, bacterial cultures devoid of heavy metals or oxyanions served as control media. All the experiments were performed in triplicate. The lowest concentration of toxic heavy metals/oxyanions, which prohibited bacterial growth, was considered as MIC value.

Morphological, biochemical, physiological, and Molecular characterization of the arsenite-tolerant bacterium

The morphological characterizations of the selected arsenite-tolerant bacterial isolate were observed regarding colony size, shape, margin, elevation, chromogenesis, surface texture, and optical details. For biochemical characterizations, a range of experiments such as Gram staining, oxidase test, catalase test, and motility were performed following standard protocols after 24 hours of incubation at 37 °C on MH-10 agar (Garrity 2007). Physiological studies were conducted by assessing bacterial growth in MH-10 broth media; salinity, temperature, and pH sensitivity were surveyed across different salinity ranges (0–23% (w/v)), temperatures (20–45 °C), and pH levels (5.0–8.0). Genomic DNA was extracted using Marmur's method (Marmur 1961) with specific modifications for molecular identification. These modifications included the digestion of the peptidoglycan-rich cell wall with lysozyme (10 mg/mL), which facilitates the breakdown of cell wall components. Subsequently, a 10% (w/v) Sodium dodecyl sulfate (SDS) solution was employed to disrupt the cell membranes and denature proteins. Proteinase K, a serine protease, was also utilized to effectively digest various proteins within the cell membrane and cytoplasm, including DNases (Mekonnen et al. 2024). The quality of the extracted genomic DNA was confirmed by 1% (w/v) agarose gel electrophoresis (Marmur 1961). The bacterial 16S rRNA gene was amplified using the isolated genomic DNA as template DNA, with 10 ng of genomic DNA in the PCR reaction. The universal bacterial primers 27F (5´-AGAGTTTGATCCTGGCTCAG-3') and 1492R (5´-GGTTACCTTGTTACGACTT-3') were utilized. PCR amplification of the 16S rRNA gene was carried out in a 30 µL reaction mixture containing 0.2 mM of each deoxynucleoside triphosphate (dNTP), 1 µM of primers 27F and 1492R, 10 ng of genomic DNA template, and one unit Taq DNA polymerase with its supplied 1x buffer (Fermentas, Hanover, Germany). The PCR reaction was performed according to the following program: initial denaturation at 95 °C for 5 minutes, followed by 30 cycles of denaturation at 94 °C for 1 minute, primer annealing at 60 °C for 1 minute, extension at 72 °C for 1 minute, and final extension at 72 °C for 10 minutes. PCR products were analyzed on a 1% agarose gel and sent to Macrogen Inc. (South Korea) for sequencing. The obtained sequences were identified based on 16S rRNA gene sequence similarities using the EzBioCloud web server (http://www.ezbiocloud.net/) (Yoon et al. 2017). The retrieved data were aligned using ClustalX2, and the phylogenetic tree was plotted using the neighbor-joining algorithm with the Tamura-Nei model in MEGA 11 software. Bootstrap analysis with 1000 replicates was conducted to assess the confidence level of the phylogenetic

tree. The 16S rRNA gene sequence obtained in this study has been deposited in NCBI GenBank under accession number PV569432.

Effect of different parameters on arsenite tolerance

The impact of different parameters such as pH, temperature, and NaCl concentration on the tolerance of selected bacterium to arsenite was determined.

Effect of sodium chloride concentrations

To determine the effect of different NaCl concentrations on the tolerance of selected bacterium toward arsenite, 0.4% (v/v) of the overnight grown log phase culture was inoculated in 20 mL fresh SW-10 media amended with different concentrations of NaCl (0, 1, 2, 3, 4, 5, 6, 7, 7.5, and 8%) (w/v) and 1 mM of sodium arsenite. All flasks were incubated at 37 °C and 150 rpm in a shaking incubator (Precise shaking incubator, WiseCube WIS-10R, Korea). Control flasks without arsenite were also prepared for each NaCl concentration. The cultures' optical density (OD) was measured at a wavelength of 600 nm by a UV-visible spectrophotometer (Shimadzu UV160U, Japan) at 0, 8, 24, 48, and 72 h of incubation. The experiment was carried out three times to ensure reproducibility.

Effect of temperature

To assess the effect of different temperatures on the arsenite tolerance of the isolated strain, 20 mL of SW-10 broth amended with 1 mM arsenite was inoculated with 0.4% (v/v) of overnight culture and incubated at a range of temperatures from 20 to 45 °C. The growth of the bacterial isolate was determined after 0, 8, 24, 48, and 72 h of incubation by measuring the optical density at 600 nm using a UV-vis spectrophotometer. The experiment was performed in triplicate. The SW-10 broth devoid of arsenite was used as a control.

Effect of pH

For determination of the effect of different pH on the tolerance of the selected bacterium to arsenite, 0.4% (v/v) of the overnight bacterial culture was inoculated into SW-10 broth supplemented with 1 mM arsenite adjusted to pH 5.0–8.0 and incubated at 37 °C on 150 rpm. After 0, 8, 24, 48, and 72 h of incubation, the optical density (OD) was taken at 600 nm using a UV-vis spectrophotometer. Also, SW-10 medium devoid of arsenite was prepared and used as a control. The experiment was performed in triplicate.

Effect of arsenite on the growth of the isolated strain

To determine the effect of different arsenite concentrations on the growth behavior of the selected bacterial isolate, 0.4% (v/v) of the overnight log phase culture was inoculated in 20 mL of SW-10 broth amended with different arsenite (0–5 mM) concentration and incubated at 37 °C, 150 rpm for 72 h in shaking incubator. The growth of the isolated strain was determined by measuring absorbance at 600 nm at a regular time interval (0, 4, 8, 24, 48, 72 h) using a UV-visible spectrophotometer. The experiment was carried out in triplicate.

Arsenite Removal Assay

The silver diethyldithiocarbamate (SDDC) method was employed to determine the total inorganic arsenic concentration (comprising both As^{3+} and As^{5+}) in the media. In this assay, the isolated bacterial strain *O. picturae* strain LW102 was inoculated into SW-10 broth containing 1 mM arsenite, with an additional control group lacking arsenite. The cultures

were incubated at 37°C with shaking at 150 rpm for 48 hours. Following incubation, bacterial cells were separated from the media by centrifugation at 8000 rpm for 10 minutes. The supernatant was collected for analysis (Jebelli et al. 2018; Dey et al. 2016; Tavoosi et al. 2024). The total arsenic concentration in the supernatant was evaluated using the SDDC method, which involves the formation of a colored complex with arsenic species that can be quantified spectrophotometrically. It is important to note that further speciation analysis, such as HPLC-ICP-MS, would provide a more comprehensive understanding of arsenic transformation and removal mechanisms; however, this was not conducted in the present study (Sel et al. 2026).

Fourier-transformed infrared (FTIR) spectroscopy

FTIR spectroscopy was used to identify the function of some chemical groups present in the bacterial cell. The overnight-grown log phase culture was inoculated in SW-10 broth supplemented with 1 mM arsenite and in media without arsenite and incubated at 37 °C, 150 rpm for 48 h. The cell pellet was harvested by centrifugation at 8000 rpm for 10 min and rinsed with 0.1 M phosphate buffer saline (pH 7.4). The cell pellet was dried in an incubator at 45 °C for 48 h. The dried cell pellet was compressed into translucent sample disks and fixed in the FTIR spectrometer (Tensor 27, Bruker, USA) for analysis.

Scanning electron microscopy (SEM) with electron dispersive X-ray spectroscopy (EDS) analysis

To examine the effect of arsenite on morphological changes in the cells, scanning electron microscopy (SEM) was used. The bacterial isolate was cultured in SW-10 broth (with 2 mM arsenite and without arsenite as control) and incubated at 37 °C, 150 rpm for 48 h. The cells were harvested by centrifugation at 8000 rpm for 10 min. The cell pellet was washed thrice with 0.1 M PBS (pH 7.4). A bacterial smear was prepared on coverslips and subsequently fixed using 2.5% glutaraldehyde overnight at 4 °C. The cells were dehydrated in increasing alcohol concentrations 20–100% (v/v) series and dried. The samples were mounted, sputtered with gold particles, and finally observed under a 25 kV Scanning Electron Microscope. Furthermore, the element analysis was examined by energy dispersive X-ray spectroscopy (EDX) (SEM QUANTA 200 FEI, USA).

Transmission electron microscopy (TEM) analysis

Transmission electron microscopy (TEM) confirmed the intracellular accumulation of As-containing compounds in and around the bacterial cells. For TEM samples, cells were grown in arsenite-free SW-10 broth and in SW-10 broth supplemented with 2 mM of arsenite at 37 °C, 150 rpm for 48 h. The bacterial cells were harvested by centrifugation at 8000 rpm for 10 min and washed thrice with PBS (phosphate buffer saline) (pH 7.4). The cell pellet was fixed using glutaraldehyde solution (2.5%) and dehydrated with graded ethanol series. The sample was embedded in epoxy resin, sectioned, and analyzed using a Transmission electron microscope (TEM Philips EM208S 100KV, Netherlands).

Statistical analysis

All experiments were performed in triplicate or more, and the data obtained were expressed as means ± standard deviation (SD). Differences between control and test groups were analyzed by one-way ANOVA, and $p < 0.05$ were considered statistically significant.

Theory and Calculation

The increasing prevalence of heavy metal pollution, particularly in arid and semi-arid regions like the Lut Desert, necessitates the exploration of bioremediation strategies that leverage the unique capabilities of halophilic and halotolerant bacteria. These microorganisms possess specialized adaptations that allow them to thrive in high-salinity environments while also exhibiting resistance to toxic heavy metals, including arsenic. The mechanisms of arsenic tolerance in bacteria can involve various biochemical pathways, including arsenate reduction, arsenite oxidation, and the

efflux of toxic compounds. Arsenic exists primarily in two oxidation states: arsenate (As^{5+}) and arsenite (As^{3+}). The latter is more toxic and soluble, posing a significant risk to ecosystems and human health. Understanding the biochemical pathways that enable bacteria to detoxify arsenite is crucial for developing effective bioremediation techniques. The ability of halophilic bacteria to oxidize arsenite to less toxic forms can be harnessed to mitigate arsenic pollution in saline environments. Moreover, the physicochemical parameters influencing bacterial growth and arsenite resistance, such as salinity, pH, temperature, and nutrient availability, must be systematically evaluated. These factors can significantly affect microbial metabolism and the efficiency of bioremediation processes. Advanced analytical techniques such as Fourier Transform Infrared (FTIR) spectroscopy, Scanning Electron Microscopy with Energy Dispersive X-ray Spectroscopy (SEM-EDS), and Transmission Electron Microscopy (TEM) provide insights into the structural and compositional changes in bacterial cells under arsenite stress, facilitating a deeper understanding of resistance mechanisms.

To evaluate the effectiveness of arsenite removal by the selected bacterial strain, we can measure the initial concentration of arsenite (C_o) and the final concentration after incubation (C_f). The percentage removal can be calculated as:

Percentage Removal = (((C_o - C_f)/C_o)) × 100

These calculations will provide quantitative insights into the bioremediation potential of the isolated strains under varying environmental conditions. By correlating growth rates and arsenite removal efficiencies with physicochemical parameters, we can identify optimal conditions for bioremediation applications in saline environments affected by heavy metal pollution.

Results and discussion

Isolation and selection of arsenite-tolerant bacteria

Table 1 presents the results of the physicochemical analysis of the soil samples. Among 16 morphologically different isolated halophilic/halotolerant bacteria from the Lut Desert, two bacterial isolates that could grow in 5 mM arsenite were considered arsenite-tolerant bacteria and selected for further investigation.

Minimum Inhibitory Concentration (MIC) of arsenite-tolerant halophilic/halotolerant isolates toward arsenic oxyanions and other heavy metals

The selected isolates, LW102 and LW105, exhibited remarkably high tolerance toward arsenate with a MIC value of 800 mM in SW-10 medium. However, their tolerance to arsenite was significantly ($p < 0.05$) lower, and they were able to grow in the presence of 30 and 10 mM of arsenite, respectively. Keep in view that arsenite toxicity is 25–60 times more than arsenate; therefore, the bacterial resistance to As^{3+} should be significantly lower than As^{5+} (Shukla et al. 2020). Arsenite and arsenate tolerance in solid media have been reported in various bacterial strains by researchers (Mujawar et al. 2019, 2021; Sher et al. 2020, 2022; Banerjee et al. 2021; Satyapal et al. 2018; Mandal et al. 2022). However, information on the bacterial tolerance potential toward arsenic oxyanions in high NaCl concentrations is scarce. Since many saline/hypersaline natural environmental systems and industrial effluents are enriched or affected by heavy metals or oxyanions, the assessment of bacterial heavy metal/oxyanion tolerance for remediation of these kinds of environments should be considered in the presence of high salinity (Voica et al. 2016; Tavoosi et al. 2023; Amoozegar et al. 2019).

Both isolates were able to tolerate selenite (Se^{4+}), lead (Pb^{2+}), cadmium (Cd^{2+}), and chromium (Cr^{6+}); however, the strain LW102 showed notably high tolerance to selenite and cadmium compared to strain LW105 ($p < 0.05$). The MIC values of

the arsenite-tolerant bacteria to arsenic oxyanions and seven heavy metals/oxyanions are given in Table 2. The strain LW102 showed remarkable tolerance to selenite (Se^{4+}) compared to previous studies and survived in 1200 mM of Se^{4+}. Guven et al. (Guven et al. 2013) reported that among 20 extremely halophilic bacteria and archaea, only one strain showed the highest tolerance to selenite, and it could tolerate up to 25 mM. In another study, *Halomonas* sp. strain MAM could tolerate selenite in the nutrient agar containing 8% NaCl (w/v) up to 200 mM (Kabiri et al. 2009). Amoozegar et al. (Amoozegar et al. 2005) showed that all 10 isolated moderately halophilic spore-forming bacilli could tolerate selenite, and strain B1 had the highest MIC value of 40 mM toward it. In a recent study, Sher et al. (Sher et al. 2020) reported that *Staphylococcus* sp. strain AS6 resisted selenite up to 4 mM in an MS-broth medium. Selenium is a trace element and essential at low concentrations for all living beings, but at high concentrations, it is toxic, and there is a slight difference between its essential and toxic doses (Fordyce 2009). In addition, the strain LW102 showed a considerably high tolerance to cadmium (8 mM) in the presence of high NaCl concentration. Cadmium has no biological function and is potentially toxic to humans, animals, plants, and microorganisms (Voica et al. 2016; Genchi et al. 2020). Various studies have investigated cadmium tolerance in different or halophilic bacteria; however, strain LW102 had a higher MIC of Cd^{2+} than the previous reports (Satyapal et al. 2018; Sher et al. 2020, 2023; Mujawar et al. 2021; Mandal et al. 2022; Amoozegar et al. 2005). Therefore, the strain LW102 could not only tolerate high concentrations of arsenate and arsenite but also demonstrate remarkable tolerance to selenite and cadmium and help remove these toxic metals/oxyanions from salt-affected soils or waters.

Table 2
MIC values of the selected isolates against arsenic oxyanions and other heavy metals, compared to those of previously reported strains

Samples	Geographical coordination	Average temperature (°C)	Average pH	Average salinity (%)	Electrical conductivity (μS/cm)	Color	Texture
W7	30°, 50´, 00.10´´ N 61°, 40´, 00.06´´E	40	7.3	23	1100±34.3	Light brown	Sandy
W8	29°, 48´, 59´´N 59°, 04´, 04´´E	42	7.5	30	1703±16.3	Brown	Sandy-loamy
W9	30°, 50´, 30.62´´ N 61°, 09´, 32.83´´E	40	7.6	32	1908±23.6	Dark brown	Sandy-loamy
W10	29°, 48´, 46.2´´ N 59°, 04´, 07´´E	40	7.5	23	1202±22.1	Light brown	Sandy

Since the strain LW102 showed the highest resistance to arsenite in the solid medium, it was subjected to MIC evaluation of arsenite in the liquid medium. The observed MIC value of arsenite was significantly lower compared to the solid medium. Moreover, the bacterial strain grew merely in the presence of 4 mM arsenite in the SW-10 broth medium.

Lower tolerance to arsenite and other heavy metals/oxyanions in the liquid media compared to solid media has been reported by different researchers (Mujawar et al. 2021; Aguilar et al. 2020).

Characterization and identification of arsenite-tolerant bacterial strain LW102

The isolated strain formed medium, irregular, cream, flat, opaque colonies with entire margins and rough surface texture on MH-10 agar. Also, strain LW102 was a Gram-stain-positive, motile, spore-forming rod that was positive for catalase and oxidase tests. Arsenite tolerance potential is reported in Gram-positive and Gram-negative bacteria; however, it is most common in Gram-positive bacteria (Dey et al. 2016; Sher et al. 2022). The findings suggest that strain LW102 can thrive in diverse environmental conditions. It demonstrated growth within a salinity range of 1 to 23% (w/v) NaCl concentration, with optimal growth occurring at 7.5% (w/v) NaCl ($p < 0.05$). Since strain LW102 could not grow in the culture medium without NaCl, the presence of Na^+ ions was essential for its growth, classifying it as a halophilic bacterium (Ventosa et al. 1998). The optimum temperature and pH required for growth were 37 °C and 7.5, respectively ($p < 0.05$). However, the strain LW102 grew at all the tested temperatures (20, 25, 30, 35, 37, 40, and 45 °C), and pH values ranged from 5.0 to 8.0 (Fig. 1). The taxonomic identity of the halophilic bacterial isolate was confirmed through analysis of 16S rRNA gene sequences on EzBiocloud. It showed the highest homology between the isolate LW102 and *Oceanobacillus picturae*. Figure 2 shows the neighbor-joining phylogenetic tree of strain LW102, which will be called *Oceanobacillus picturae* strain LW102 in this study. Our phylogenetic analysis substantiates its classification at the genus level; however, it is noteworthy that there are currently no documented instances of arsenite tolerance within this genus. Most isolated arsenite-tolerant strains are related to the genus *Bacillus*. However, numerous phylogenetically diverse bacteria have been reported as arsenite-tolerant. They are isolated from various environmental sources such as saline or non-saline soil and water chemical industry wastewater (Dey et al. 2016; Mujawar et al. 2019, 2021; Sher et al. 2020, 2022; Mandal et al. 2022; Biswas et al. 2019). To further substantiate our claim regarding the novelty of *O. picturae* strain LW102's arsenite tolerance, additional research is warranted to elucidate the roles of specific genes implicated in this mechanism. This includes key arsenite resistance genes such as *aoxAB* and components of the ars operon, which may be identified through genomic database analyses.

Effect of different NaCl concentrations, temperatures, and pH on the arsenite-tolerance potential of the Oceanobacillus picturae strain LW102

Without arsenite, *O. picturae* strain LW102 could grow optimally at a salinity of 7.5%, temperature of 37 °C, and pH of 7.5. The strain showed a similar pattern in the presence of 1 mM arsenite. It grew at a salt concentration range of 1–8% with an optimum of 7.5% ($p < 0.05$) and temperature of 35, 37, and 40 °C with an optimum of 37 °C ($p < 0.05$); however, its optimum pH value was 7.0 ($p < 0.05$) (Fig. 3). Since in the presence and absence of arsenite in the medium, *O. picturae* strain LW102 could grow optimally at 7.5% NaCl, and its growth rate decreases at higher arsenite concentrations; thus, it could be interpreted that NaCl concentrations do not interfere with the tolerance of *O. picturae* strain LW102 to As^{3+}, and the decrease in growth rate may be attributed to As^{3+} toxicity effects. In a previous study, *Halomonas elongata* strain SEK2 could grow optimally at 15% NaCl (w/v) without As^{3+} in the SW medium. However, in the presence of As^{3+}, its optimal growth was observed at 8% NaCl (w/v) (Tavoosi et al. 2024). Generally, it is assumed that the simultaneous presence of the As^{3+} and NaCl concentrations up to certain limits in the medium could negatively affect bacterial growth (Sher et al. 2021a, b). Among environmental factors, temperature and pH are two important variables that play major roles in bacterial growth and heavy metal or oxyanion tolerance. The maximum growth of *O. picturae* strain LW102 was obtained at pH 7.0 and 37 °C, consistent with previously reported results (Sher et al. 2021a; Tanmo et al. 2018).

Effect of arsenite on the growth behavior of the halophilic bacterial O. picturae strain LW102

The *O. picturae* strain LW102 growth curve under arsenite stress conditions showed a sigmoidal growth pattern, and increasing concentrations of arsenite led to the extension of its lag phase and growth inhibition (Fig. 4). Under arsenite stress in the surrounding environment, bacteria employ different mechanisms to survive. Therefore, the lengthened lag phase could be due to the acclimatization of the bacterial isolate to the presence of arsenite in the environment.

Removal of Arsenite by Oceanobacillus picturae Strain LW102

The SDDC method was employed to assess arsenite oxidation and the removal potential of *O. picturae* strain LW102. Arsenite oxidation is one of the resistance mechanisms that bacteria utilize to convert arsenite (As^{3+}) into a less toxic form, arsenate (As^{5+}). Since bacterial tolerance to arsenate is significantly higher than that of arsenite, bacteria can more effectively manage the toxic effects of arsenite. The process of arsenite oxidation occurs in the periplasmic space, mediated by arsenite oxidase genes located within the aox operon. This operon also encodes other essential components, including a sensor kinase that detects external arsenite and aquaglyceroporins, which facilitate the transport of arsenite into the cell (Dey et al. 2016).

The results from the SDDC test indicated that after 48 hours of incubation, *O. picturae* strain LW102 successfully oxidized arsenite to arsenate. In this study, we were unable to employ the silver nitrate screening assay, commonly used for determining arsenite oxidizing ability, due to interactions between NaCl and $AgNO_3$, which resulted in AgCl precipitation. However, the SDDC method clearly demonstrated the rapid transformation of arsenite to arsenate (Jebelli et al. 2018). The arsenite bioremoval potential of the *O. picturae* strain LW102 was evaluated using the SDDC method. After 48 hours in SW7.5% medium supplemented with 1 ± 0.02 mM arsenite, strain LW102 successfully reduced the arsenite concentration to 0.25 ± 0.07 mM (Fig. 4b), achieving a reduction of approximately 80% (Fig. 4c). It is important to clarify that this 80% reduction refers specifically to the oxidation of As^{3+} to As^{5+}, rather than a total reduction in arsenic concentration due to removal mechanisms such as precipitation or biosorption. The SDDC method quantifies total inorganic arsenic (comprising both As^{3+} and As^{5+}), thus distinguishing between oxidation and actual removal from solution requires additional analytical techniques. Future studies utilizing methods such as HPLC-ICP-MS would be ideal for speciation and confirming the transformation of arsenite (Dey et al. 2016). In addition to oxidation, bacteria can employ various detoxification mechanisms under arsenite stress, including bioaccumulation, biosorption, and efflux pumps to mitigate arsenite concentrations in their environment (Jebelli et al. 2018). In addition, *O. picturae* strain LW102 is a Gram-positive bacterial strain, and it is considered that Gram-positive bacteria are more resistant to toxic heavy metals or oxyanions as they have a thicker cell wall, which inhibits the entry of toxic metals or oxyanions into the cell and prevent DNA damage and other internal organelles (Dey et al. 2016).

Fourier transform infrared (FTIR) spectroscopic analysis

FTIR spectroscopic analysis revealed significant shifts and changes in peak intensity within the 500–4000 cm^{-1} range for *O. picturae* strain LW102 treated with 1 mM arsenite compared to the control (Fig. 5). These spectral changes can be attributed to various functional groups involved in arsenite adsorption, accumulation, or uptake into the bacterial cell (Table 3). Notably, a peak shift from 3270.56 cm^{-1} to a higher wavenumber of 3272.87 cm^{-1} was observed, indicating the stretching of amides (N-H) following arsenite exposure. Conversely, peaks at 3416.33 cm^{-1} and 2853.65 cm^{-1}, corresponding to the O-H stretch of hydroxyl groups, O-H stretch of carboxylic acids, and C-H stretch of alkanes, shifted to lower wavenumbers upon arsenite treatment.

Table 3
IR peaks shift, indicating the presence of functional groups on the surface of *Oceanobacillus picturae* strain LW102

Arsenooxyanions and Heavy metals	**MIC value (in mM)**					
	LW102	**LW105**	***Bacillus flexus* strain SSAI1 (Mujawar et al. 2021)**	***Klebsiella pneumoniae* strain SSSW7 (Mujawar et al. 2019)**	***Staphylococcus* sp. strain AS6 (Sher et al. 2020)**	***Halomonas elongata* strain SEK2 (Tavoosi et al. 2024)**
Arsenate (As^{5+})	800	800	-	-	150	800
Arsenite (As^{3+})	30	10	25	21	25	40
Selenite (Se^{4+})	1200	600	-	-	-	-
Lead (Pb^{2+})	1	1	-	-	-	2
Cadmium (Cd^{2+})	8	1	-	-	-	1
Copper (Cu^{2+})	-	-	-	-	-	-
Zinc (Zn^{2+})	-	-	-	-	-	-
Chromium (Cr^{6+})	1	1	-	-	-	1
Mercury (Hg^{2+})	-	0.5	-	-	-	-

Untreated cells (cm^{-1})	Arsenite treated cells (cm^{-1})	Band assignments
3416.33	3414.47	O-H stretch of hydroxyl groups
3270.56	3272.87	N-H stretch of amides
2853.65	2853.45	O-H stretch of carboxylic acids, C-H stretch of alkanes
1796.65	1797.86	C-O stretch of alcohol and carboxylic acids
1642.26	1643.65	-C = C stretch of alkenyl
1552.80	1550.59	N-H bend of 1° amine, N-O stretch of nitro compounds
1495.88	1495.40	C = C-C stretch of aromatic ring
1457.20	1458.35	C-H bend of methylene and methyl groups
1415.39	-	-C-H bend of alkane
1374.64	1374.79	C-H bend of methyl groups
1322.83	1322.77	C-N stretch of aromatic primary amines
1278.07	1277.92	C-N stretch of aromatic amines, C-O stretch of alcohols, carboxylic acids, esters
1246.06	1246.56	P = O stretch of phosphates
1189.00	1153.92	C-O stretch of esters, C-N stretch of aliphatic amine
1108.20	1104.40	C-O stretch of alcohol, carboxylic acids, esters, ethers
1062.29	1061.27	C-O stretch of alcohol, carboxylic acids, esters, ethers, C-N stretch of aliphatic amines
1005.38	1007.60	P-O-C stretch of aliphatic phosphates
923.35	-	-C-H bend of alkenes
882.51	881.90	C-H bend of aromatics
849.29	-	C-H bend of aromatics
790.46	790.69	C-Cl stretch of aliphatic chloro compounds
698.98	698.02	C-Br stretch of alkyl halides
629.94	628.52	C-Cl and C-Br stretch of alkyl halides, C-H bend of alkynes

FTIR spectra also demonstrated peak shifts in the regions of 1800 – 1500 cm^{-1} and 1500 – 1200 cm^{-1}, which are associated with proteins, peptides, fatty acids, and phosphates in the bacterial cell wall and membrane. These shifts indicate interactions between arsenite ions and specific chemical moieties present in the bacterial cells (Naumann et al. 1991). Additionally, *O. picturae* strain LW102 exhibited multiple peak shifts between 1200 and 900 cm^{-1}, including transitions from 1189.00 to 1153.92 cm^{-1}, 1108.20 to 1104.40 cm^{-1}, 1062.29 to 1061.27 cm^{-1}, and 1005.38 to 1007.60 cm^{-1} in the presence of arsenite. These changes correspond to the stretching of esters (C-O), aliphatic amines (C-N), alcohols, carboxylic acids, ethers (C-O), aliphatic phosphates (P-O-C), and bending of alkenes (-C-H). The presence of these functional groups suggests that components of the bacterial cell wall are actively involved in the interaction with arsenite (Tanmoy et al. 2018; Oust et al. 2004). Furthermore, Omoike and Chorover (Omoike and Chorover 2004)

highlighted that phosphodiester group peaks in the region of 1132 to 994 cm^{-1} may enhance the negative charge on bacterial membranes, facilitating the attraction of cationic metal ions from the environment. The observed peak shifts in the region of 900 to 600 cm^{-1} indicated bending of aromatics (C-H), alkynes (C-H), and stretching of aliphatic chloro compounds (C-Cl) and alkyl halides (C-Br). Based on our FTIR spectroscopy results, it is evident that several functional groups on the surface of *O. picturae* strain LW102's cell wall interact with arsenite, suggesting potential mechanisms of biosorption or bioaccumulation (Mujawar et al. 2021; Balan et al. 2018). To clarify this distinction, we propose that the shifts observed may indicate biosorption primarily through binding to cell surface groups; however, further investigation is warranted to ascertain whether internalization occurs, indicative of bioaccumulation. Previous studies have reported similar functional groups in various bacterial strains interacting with arsenite, including *Bacillus flexus* strain SSAI1, *Microbacterium* sp. strain 1S1, *Staphylococcus* sp. strain AS6, *Klebsiella pneumoniae* strain SSSW7, *Bacillus aryabhattai* strain NBRI014, and *Arthrobacter* sp., reinforcing our findings (Mujawar et al. 2021, 2019; Sher et al. 2020, 2022; Singh et al. 2016; Prasad et al. 2013).

SEM and EDX Analysis

The scanning electron microscopy (SEM) micrograph of *O. picturae* strain LW102 exposed to 2 mM of arsenite indicated no prominent changes in the size and morphology of the bacterial cells compared to the control cells without arsenite, as shown in Fig. 6a and b. This observation suggests that *O. picturae* strain LW102 may efficiently manage arsenite through oxidation and efflux mechanisms. Specifically, as arsenite enters the cell, it is converted to less toxic arsenate and subsequently extruded from the cell, resulting in no significant alterations in cell size or morphology. This mechanism could indicate the presence of active efflux systems within the bacterial cells, which help maintain cellular integrity under arsenite stress. Previous studies have reported varying responses among different bacterial strains, including increases or reductions in cell size and morphological changes when exposed to arsenite (Mujawar et al. 2019, 2021; Mandal et al. 2022; Sher et al. 2021b, 2024). Furthermore, energy-dispersive X-ray spectroscopy (EDX) results confirmed the presence of arsenic on the surface of *O. picturae* strain LW102, with peaks observed in treated cells but absent in untreated controls (Figs. 6c and d). This suggests surface interactions between arsenic and the bacterial cells (Dey et al. 2016; Tavoosi et al. 2024).

TEM Analysis

The transmission electron micrograph of *O. picturae* strain LW102 exposed to 2 mM arsenite revealed the presence of electron-dense deposits throughout the cytoplasm, whereas untreated cells exhibited a clear cytoplasm, as shown in Fig. 7. The observed intracellular structures indicate that *O. picturae* strain LW102 employs intracellular sequestration as an additional strategy to mitigate the toxic effects of arsenite. These electron-dense deposits likely represent accumulated arsenite or its derivatives, suggesting a complex interplay between detoxification mechanisms. Similar findings of condensed cytoplasm and dark periplasmic regions have been reported in previous studies, indicating that these changes may be attributed to intracellular arsenite accumulation (Mujawar et al. 2019, 2021; Banerjee et al. 2011).

Proposed Model for Arsenic Handling

In synthesizing these seemingly contrasting results from SEM and TEM analyses, we propose a coherent model for how *O. picturae* strain LW102 manages arsenic stress. It appears that this bacterium employs a combination of oxidation, efflux, and intracellular sequestration mechanisms to handle arsenite effectively. Upon exposure to arsenite, the bacteria likely oxidize it to arsenate, which is then extruded through efflux systems to prevent cellular damage. Concurrently, some arsenite may enter the cell and be sequestered within electron-dense deposits in the cytoplasm, providing a means of detoxification and storage. This multifaceted approach allows *O. picturae* strain LW102 to thrive in environments contaminated with arsenic while minimizing its toxic effects. This proposed model aligns with findings from other studies that have highlighted similar strategies employed by various bacterial strains in response to arsenic

stress (Mujawar et al. 2019, 2021; Sher et al. 2020, 2022; Prasad et al. 2013). Further investigations are warranted to elucidate the specific molecular mechanisms underpinning these processes in *O. picturae* strain LW102.

Conclusion

The application of microorganisms as a sustainable biological method for remediating heavy metal and oxyanion-contaminated water, groundwater, and soil is emerging as a promising technology. This study concludes that *Oceanobacillus picturae* strain LW102 exhibits considerable tolerance to arsenate and selenite, as well as high levels of arsenite and cadmium. Given that this strain is halophilic and requires the presence of salts, it may serve as a promising candidate for future studies on bioremediation in high-salinity environments, such as industrial effluents.

The results indicated that *O. picturae* strain LW102 can efficiently remove arsenite from the medium and oxidize arsenite (a highly toxic form) to arsenate (a less toxic form) at 37°C and pH 7.0. Investigations into the arsenite resistance mechanisms of *O. picturae* strain LW102 revealed that the isolate employs various strategies to endure adverse conditions. Notably, this investigation highlights the significance of *Oceanobacillus picturae* as an arsenite-resistant bacterium, a characteristic that has not been reported in previous studies, nor has its potential for arsenite removal been explored. Furthermore, additional research is required to elucidate the role of specific genes involved in this process, including key arsenite resistance genes such as *aoxAB* and components of the ars operon, which may be present based on genomic database analyses. Overall, the efficient oxidizing ability of *O. picturae* strain LW102 toward arsenite, its effective interactions with arsenite, notable resistance to arsenite and other heavy metals/oxyanions, and its capacity to remove arsenite in high-salt media position it as a suitable candidate for decontaminating arsenic from saline-polluted environments. Additionally, the potential application of *O. picturae* strain LW102 in field-scale bioremediation is significant. Its ability to thrive in saline conditions makes it particularly advantageous for treating contaminated sites affected by industrial activities, where both heavy metal pollution and high salt concentrations are prevalent. Future field studies could assess the efficacy of this strain in real-world scenarios, further establishing its role in sustainable bioremediation efforts.

Declarations

Acknowledgments

We thank Shubham Pandey, Bhavna Parmar, and Anjali Gupta for their helpful feedback on this manuscript.

Funding

The authors declare that no funds, grants, or other support were received during the preparation of this manuscript.

Availability of data and materials

The 16S rRNA gene sequence obtained in this study has been deposited in NCBI GenBank under accession number PV569432.

Declaration of Interest statement

The authors have no relevant financial or non-financial interests to disclose.

Author Contributions

All authors contributed to the study's conception and design. M.A. supervised the work and developed the idea. N.T. and A.S. performed the experiments and N.T., M.A., and A.A.S. analyzed and interpreted the data. N.T., A.S. and M.A.

discussed the paper and N.T. and A.S. drafted the manuscript and R.K. analyzed and interpreted the data and discussed the paper. All authors critically revised the manuscript for important intellectual content. All authors read and approved the final manuscript. All authors Agree to be accountable for all aspects of the work in ensuring that questions related to the accuracy or integrity of any part of the work are appropriately investigated and resolved.

Declaration of generative AI and AI-assisted technologies in the writing process

During the preparation of this work, the authors used ChatGPT, an AI language model developed by OpenAI, to assist with English language editing. After utilizing this tool, the authors reviewed and edited the content as needed and take full responsibility for the content of the publication.

References

1. Aguilar MC, Faria T, Pedron BL, Batista JP, Mesquita CA, Bomfeti JL, Rodrigues (2020) Isolation and characterization of bacteria from a brazilian gold mining area with a capacity of arsenic bioaccumulation. Chemosphere 240:124871–124881. https://doi.org/10.1016/j.chemosphere.2019.124871
2. Amoozegar J, Hamedi M, Dadashipour S, Shariatpanahi (2005) Effect of salinity on the tolerance to toxic metals and oxyanions in native moderately halophilic spore-forming bacilli. World J Microbiol Biotechnol 21:1237–1243. https://doi.org/10.1007/s11274-005-1804-0
3. Baati M, Siala C, Azri E, Ammar C, Dunlap M, Trigui (2020) Resistance of a *Halobacterium salinarum* isolate from a solar saltern to cadmium, lead, nickel, zinc, and copper, Antonie. Van. Leeuwenhoek. 113 (2020) 1699–1711. https://doi.org/10.1007/s10482-020-01475-6
4. Balan S, Shini KP, Krishnan M, Mohan (2018) Mercury tolerance and biosorption in bacteria isolated from Ny-Alesund, Svalbard, Arctic. J Basic Microbiol 58:286–295. https://doi.org/10.1002/jobm.201700496
5. Banerjee S, Datta D, Chattyopadhyay P, Sarkar (2011) Arsenic accumulating and transforming bacteria isolated from contaminated soil for potential use in bioremediation. J Environ Sci Health 46:1736–1747. https://doi.org/10.1080/10934529.2011.623995
6. Banerjee S, Sarkar S, Gorai A, Kabiraj R, Bandopadhyay (2021) High arsenic tolerance in *Brevundimonas aurantiaca* PFAB1 from an arsenic-rich Indian hot spring. Electron J Biotechnol 53:1–7. https://doi.org/10.1016/j.ejbt.2021.05.006
7. Bhowmik SC, Prajapati S, Kumar K, Priyanka R, Saxena (2025) Bioremediation of Arsenic metal from water and soil by Bacillus species-A review. J Integ Sci Technol 13:1038–1049. https://doi.org/10.62110/sciencein.jist.2025.v13.1038
8. Biswas V, Vivekanand A, Saha A, Ghosh A, Sarkar (2019) Arsenite oxidation by a facultative chemolithotrophic *Delftia* spp. BAs29 for its potential application in groundwater arsenic bioremediation. Int Biodeterior Biodegradation 136:55–62. https://doi.org/10.1016/j.ibiod.2018.10.006
9. Dey S, Chatterjee NK, Mondal (2016) Isolation and characterization of arsenic-resistant bacteria and possible application in bioremediation. Biotechnol Rep 10:1–7. https://doi.org/10.1016/j.btre.2016.02.002
10. Fordyce (2009) Selenium deficiency and toxicity in the environment. In: Selinus O (ed) Essentials of Medical Geology. Springer, Netherlands, pp 375–416. https://doi.org/10.1007/978-94-007-4375-5_16.
11. Garrity (2007) The Proteobacteria, part B: the Gammaproteobacteria (Vol. 2), in: Bergey's manual of systematic bacteriology, 2nd edn, Springer, New York, pp 270–282
12. Genchi MS, Sinicropi G, Lauria A, Carocci A, Catalano (2020) The effects of cadmium toxicity. Int J Environ Res Public Health 17:3782–3791. https://doi.org/10.3390/ijerph17113782

13. Guven MB, Mutlu C, Cırpan HM, Kutlu (2013) Isolation and identification of selenite reducing archaea from Tuz (salt) Lake In Turkey, J. Basic. Microbiol. 53 397–401. https://doi.org/10.1002/jobm.201200008
14. He W, Xiao J, Zeng J, Tang L, Wang (2023) Detoxification and removal of arsenite by *Pseudomonas* sp. SMS11: Oxidation, biosorption and bioaccumulation. J Environ Manag 336:117641–117649. https://doi.org/10.1016/j.jenvman.2023.117641
15. Jebelli A, Maleki MA, Amoozegar E, Kalantar F, Gharibi N, Darvish H, Tashayoe (2018) Isolation and identification of the native population bacteria for bioremediation of high levels of arsenic from water resources. J Environ Manag 212:39–45. https://doi.org/10.1016/j.jenvman.2018.01.075
16. Kabiri MA, Amoozegar M, Tabebordbar K, Gilany GH, Salekdeh (2009) Effects of selenite and tellurite on growth, physiology, and proteome of a moderately halophilic bacterium. J Proteome Res 8:3098–3108. https://doi.org/10.1021/pr900005h
17. Kalankesh S, Rodriguez-Couto A, Alami S, Khosravan M, Meshki E, Ahmadov N, Bahri (2022) Socio-Environmental Determinants and Human Health Exposures in Arid and Semi-Arid Zones of Iran—Narrative. Rev Environ Health Insights 16:11786302221089738–11786302221089748. https://doi.org/10.1177/11786302221089738
18. Lyons SA, Welch CB, Gardner A, Sharifi A, AghaKouchak M, Mashkour H, Akhani (2020) The hydrogeochemistry of shallow groundwater from Lut Desert, Iran: The hottest place on Earth. J Arid Environ 178:104143–104155. https://doi.org/10.1016/j.jaridenv.2020.104143
19. Mandal R, Sonar I, Saha S, Ahmed A, Basu (2022) Isolation and identification of arsenic resistant bacteria: a tool for bioremediation of arsenic toxicity. Int J Environ Sci Technol 19:9883–9900. https://doi.org/10.1007/s13762-021-03673-9
20. Marmur (1961) A procedure for the isolation of deoxyribonucleic acid from microorganisms. J Mol Biol 3:208–IN1. https://doi.org/10.1016/S0022-2836(61)80047-8
21. Mekonnen ME, Aspholm ED, Zegeye ED (2024) High-Quality Genomic DNA Extraction Protocol for Bacillus and Clostridium Species. Curr Protoc 4:e70027–e70039. https://doi.org/10.1002/cpz1.70027
22. Mujawar DC, Vaigankar SK, Dubey (2021) Biological characterization of *Bacillus flexus* strain SSAI1 transforming highly toxic arsenite to less toxic arsenate mediated by periplasmic arsenite oxidase enzyme encoded by aioAB genes, BioMetals. 34:895–907. https://doi.org/10.1007/s10534-021-00316-x
23. Mujawar K, Shamim DC, Vaigankar SK, Dubey (2019) Arsenite biotransformation and bioaccumulation by *Klebsiella pneumoniae* strain SSSW7 possessing arsenite oxidase (aioA) gene, BioMetals. 32:65–76. https://doi.org/10.1007/s10534-018-0158-7
24. Naumann D, Helm H, Labischinski P, Giesbrecht (1991) The characterization of microorganisms by Fourier-transform infrared spectroscopy. In: Nelson WH (ed) Modern techniques for rapid microbiological analysis. VCH, NewYork, pp 43–96
25. Nieto R, Fernandez-Castillo MC, Marquez A, Ventosa E, Quesada F, Ruiz-Berraquero (1989) Survey of metal tolerance in moderately halophilic eubacteria. Appl Environ Microbiol 55:2385–2390. https://doi.org/10.1128/aem.55.9.2385-2390.1989
26. Omoike J, Chorover (2004) Spectroscopic study of extracellular polymeric substances from *Bacillus subtilis*: aqueous chemistry and adsorption effects. Biomacromolecules 5:1219–1230. https://doi.org/10.1021/bm034461z
27. Oust T, Moretro C, Kirschner JA, Narvhus A, Kohler (2004) FT-IR spectroscopy for identification of closely related lactobacilli. J Microbiol Methods 59:149–162. https://doi.org/10.1016/j.mimet.2004.06.011
28. Patel PK, Pandey P, Martín-Ramos WT, Corns S, Varol P, Bhattacharya Y, Zhu Y (2023) A review on arsenic in the environment: bio-accumulation, remediation, and disposal. RSC Adv 13:14914–14929. https://doi.org/10.1039/D3RA02018E

29. Prasad AL, Ramanathan J, Paul V, Subramanian R, Prasad (2013) Biosorption of arsenite (As^{+3}) and arsenate (As^{+5}) from aqueous solution by *Arthrobacter* sp. Biomass. Environ Technol 34:2701–2708. https://doi.org/10.1080/09593330.2013.786137
30. Rodriguez-Castrejon AH, Serafin-Muñoz A, Alvarez-Vargas G, Cruz-Jímenez B, Noriega-Luna (2022) Isolation and molecular identification of native As-resistant bacteria: As (III) and As (V) removal capacity and possible mechanism of detoxification. Arch Microbiol 204:191–204. https://doi.org/10.1007/s00203-022-02794-0
31. Satyapal SK, Mishra A, Srivastava RK, Ranjan K, Prakash R, Haque N, Kumar (2018) Possible bioremediation of arsenic toxicity by isolating indigenous bacteria from the middle Gangetic plain of Bihar, India. Biotechnol Rep 17:117–125. https://doi.org/10.1016/j.btre.2018.02.002
32. Schneegurt (2012) Media and Conditions for the Growth of Halophilic and Halotolerant Bacteria and Archaea. In: Vreeland RH (ed) Advances in Understanding the Biology of Halophilic Microorganisms. Springer, Dordrecht, pp 35–58. https://doi.org/10.1007/978-94-007-5539-0_2.
33. Sel B, Aydoğan I, Koyuncu (2026) Determination of arsenic species in seafood samples using a combination of HPLC and ICP-MS after ultrasonic assisted sample preparation. Talanta 296:128518. https://doi.org/10.1016/j.talanta.2025.128518
34. Sher A, Ghani S, Sultan A, Rehman (2021a) Bacterial strains isolated from heavy metals contaminated soil and wastewater with potential to oxidize arsenite. Environ Process 8:333–347. https://doi.org/10.1007/s40710-020-00488-7
35. Sher S, Sultan A, Rehman (2021b) Characterization of multiple metal resistant *Bacillus licheniformis* and its potential use in arsenic contaminated industrial wastewater. Appl Water Sci 11:1–7. https://doi.org/10.1007/s13201-021-01407-3
36. Sher S, Ullah DA, Bukhari SZ, Hussain A, Rehman (2024) Evaluation of interaction among arsenic and *Brevibacterium* sp. strain CS2 and its proteins profiling. J Hazard Mater Lett 5:100119–100130. https://doi.org/10.1016/j.hazl.2024.100119
37. Sher SZ, Hussain A, Rehman (2020) Multiple resistance mechanisms in *Staphylococcus* sp. strain AS6 under arsenite stress and its potential use in amelioration of wastewater. J King Saud Univ Sci 32:3052–3058. https://doi.org/10.1016/j.jksus.2020.08.012
38. Sher SZ, Hussain MT, Cheema A, Hussain A, Rehman (2022) Efficient removal potential of *Microbacterium* sp. strain 1S1 against arsenite isolated from polluted environment. J King Saud Univ Sci 34:102066–102072. https://doi.org/10.1016/j.jksus.2022.102066
39. Shirsalimian SM, Mazidi MA, Amoozegar (2022) The Lut Desert and Its Microbial Diversity: Recent Studies and Future Research. Microbiol 91:215–224. https://doi.org/10.1134/S0026261722300014
40. Shukla KM, Sarim DP, Singh (2020) Microbe-mediated management of arsenic contamination: current status and future prospects. Environ Sustain 3:83–90. https://doi.org/10.1007/s42398-019-00090-0
41. Singh S, Gupta N, Marwa V, Pandey PC, Verma S, Rathaur N, Singh (2016) Arsenic mediated modifications in *Bacillus aryabhattai* and their biotechnological applications for arsenic bioremediation. Chemosphere 164:524–534. https://doi.org/10.1016/j.chemosphere.2016.08.119
42. Soto E, Vilo C, Aguayo P et al (2026) Mitigation of arsenic toxicity in natural waters using a bacterial biomineralizing system. Sci Rep. https://doi.org/10.1038/s41598-026-60589-5
43. Tanmoy A, Chakraborty E, Islam SK, Mukherjee (2018) Arsenic bioremediation potential of arsenite-oxidizing *Micrococcus* sp. KUMAs15 isolated from contaminated soil. Pedosphere 28:299–310. https://doi.org/10.1016/S1002-0160(17)60493-4

44. Tavoosi A, Akhavan Sepahi MA, Amoozegar V, Kiarostami (2023) Toxic heavy metal/oxyanion tolerance in haloarchaea from some saline and hypersaline ecosystems. J Basic Microbiol 63:558–569. https://doi.org/10.1002/jobm.202200465
45. Tavoosi A, Akhavan Sepahi V, Kiarostami MA, Amoozegar (2024) Arsenite tolerance and removal potential of the indigenous halophilic bacterium, *Halomonas elongata* SEK2, BioMetals. 37 1–17. https://doi.org/10.1007/s10534-024-00612-2
46. Ventosa MC, Garabito DR, Arahal (1998) Moderately halophilic gram-positive bacterial diversity in hypersaline environments. Extremophiles 2:297–304. https://doi.org/10.1007/s007920050072
47. Voica L, Bartha HL, Banciu A, Oren (2016) Heavy metal resistance in halophilic Bacteria and Archaea, FEMS. Microbiol Lett 363:14–21. https://doi.org/10.1093/femsle/fnw146
48. Yadav MW, Ansari R, Gill N, Tuteja SS, Gill (2024) Arsenic transport, detoxification, and recent technologies for mitigation: a systemic review. Plant Physiol Biochem 213:108848–108860. https://doi.org/10.1016/j.plaphy.2024.108848
49. Yang Y, Li R, Feng J, Chen HA, Alwathnani W, Xu C, Rensing (2022) Characterization of two highly arsenic-resistant *Caulobacteraceae* strains of *Brevundimonas nasdae*: discovery of a new arsenic resistance determinant. Int J Mol Sci 23:5619–5633. https://doi.org/10.3390/ijms23105619
50. Yoon SM, Ha S, Kwon J, Lim Y, Kim H, Seo J, Chun (2017) Introducing EzBioCloud: a taxonomically united database of 16S rRNA gene sequences and whole-genome assemblies. Int J Syst Evol Microbiol 67:1613–1617. https://doi.org/10.1099/ijsem.0.001755

Figures

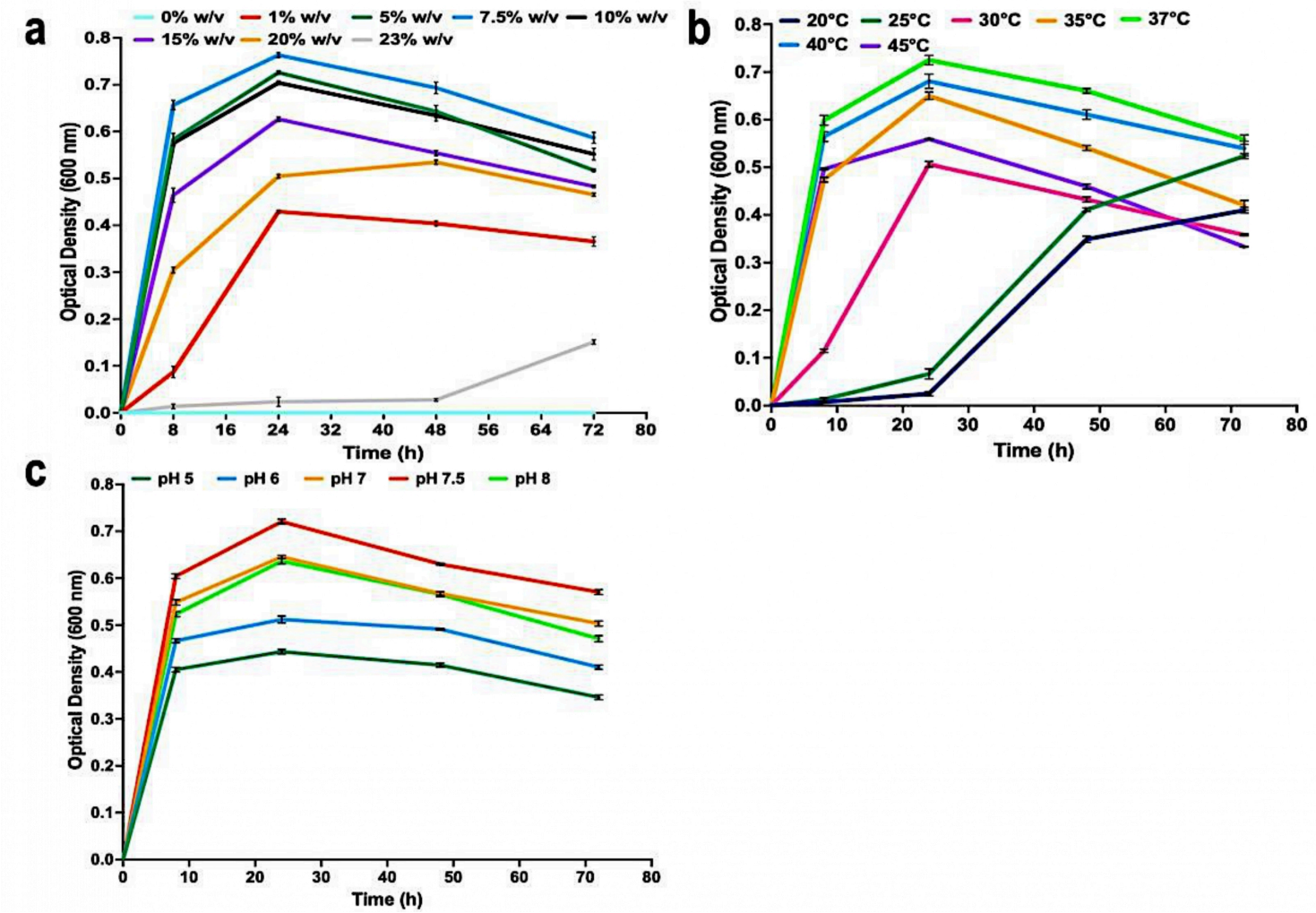

Figure 1

Growth of *Oceanobacillus picturae* strain LW102 under various conditions: (a) Salinity; (b) Temperature; and (c) pH, in the absence of arsenite

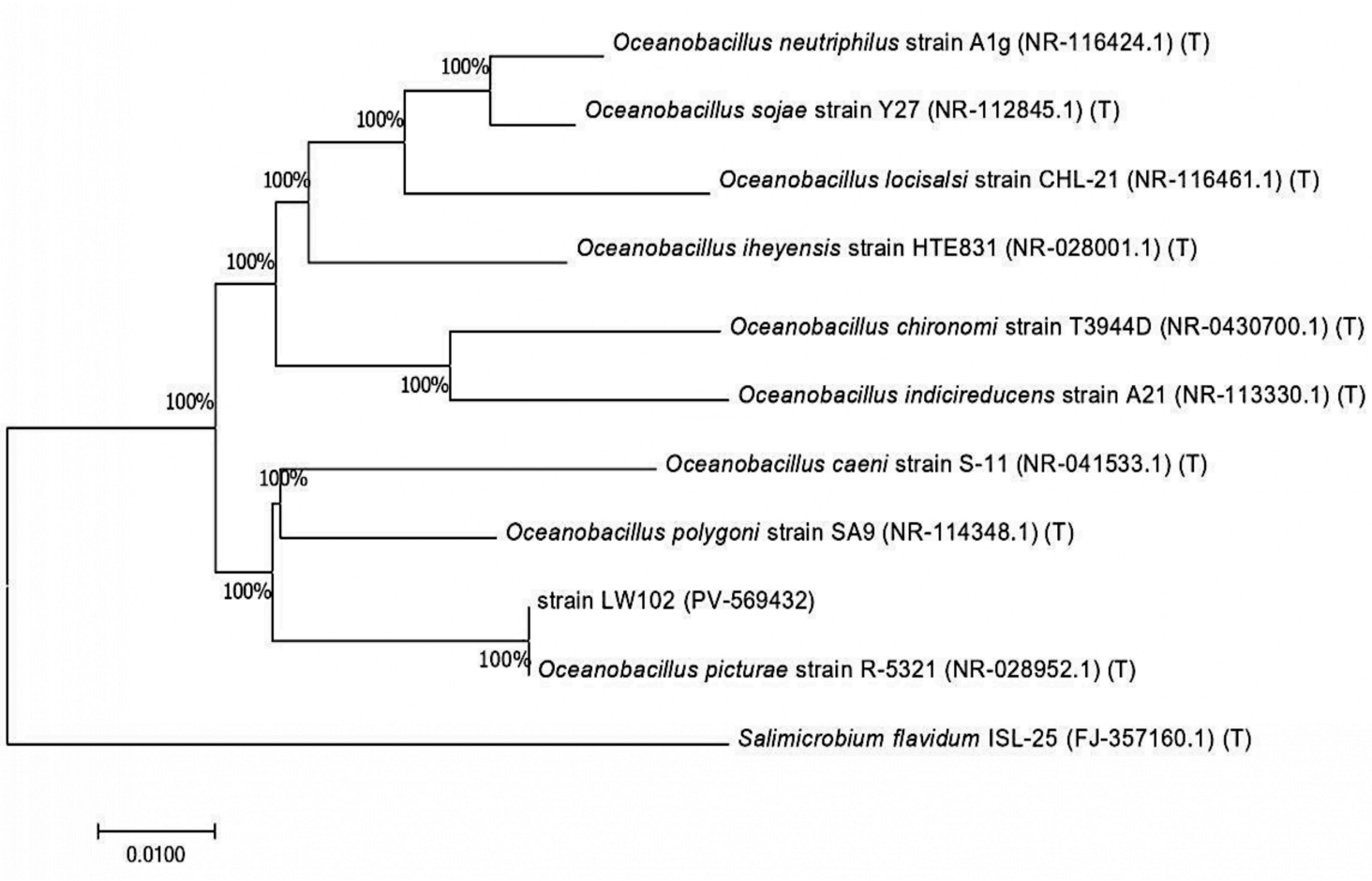

Figure 2

Phylogenetic tree based on 16S rRNA gene sequences, showing the position of strain LW102 among the other strains of the genus *Oceanobacillus.* Bootstrap values are based on 1000 replicates.

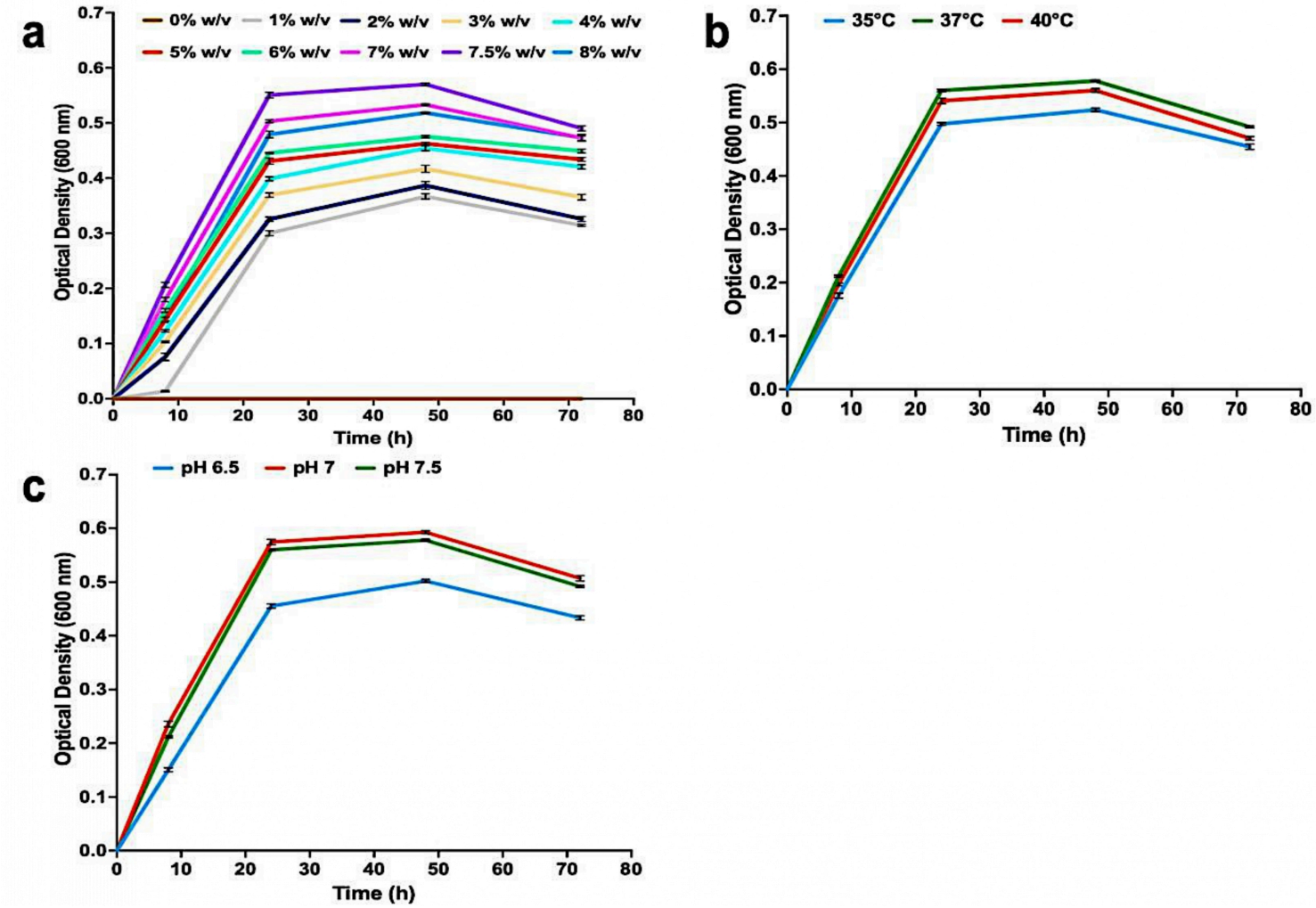

Figure 3

The growth of *Oceanobacillus picturae* strain LW102 in presence of 1mM arsenite under different conditions: (a) Salinity; (b) Temperature; and (c) pH. Error bars represent SD of triplicate measurements (n = 3)

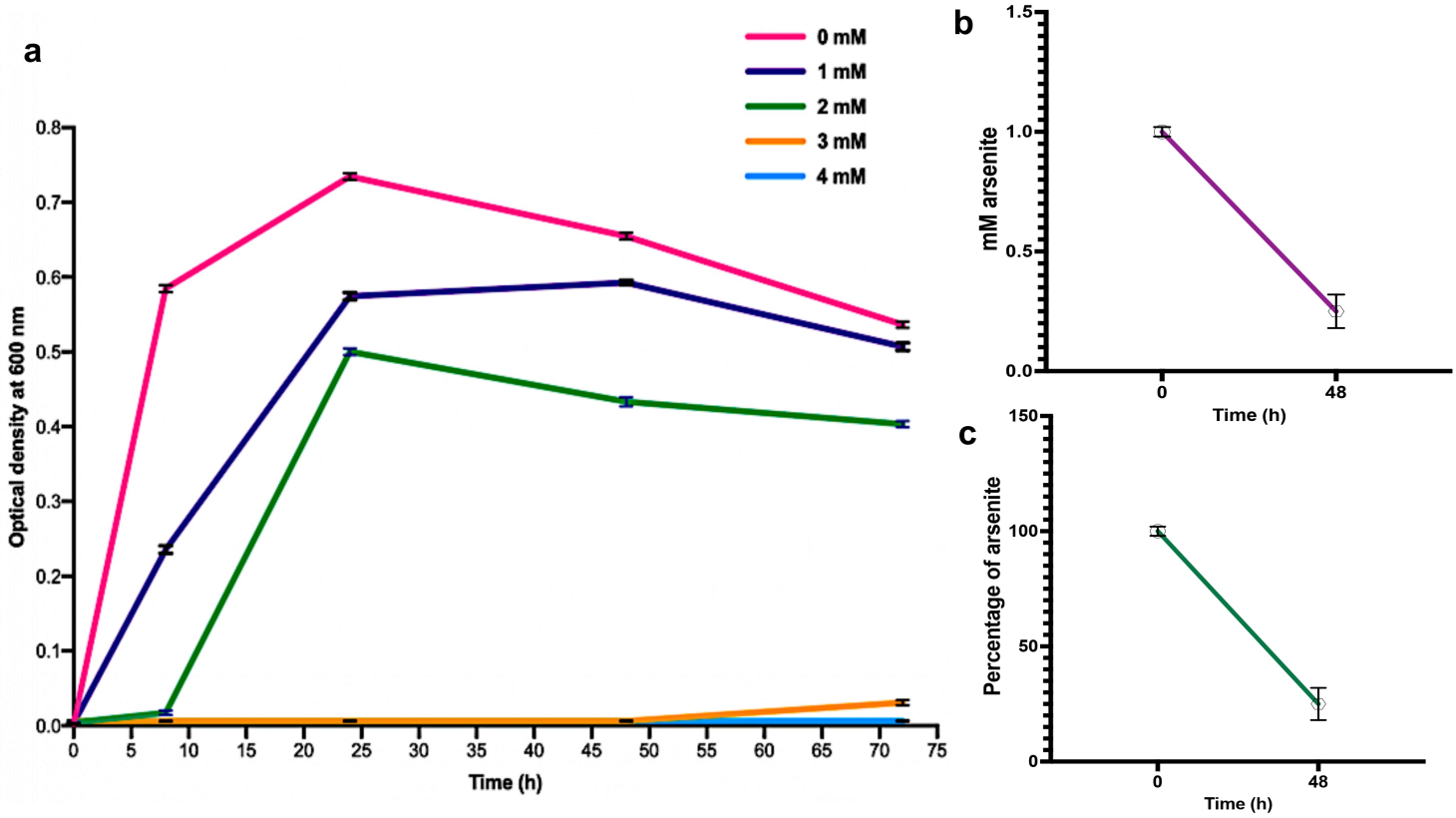

Figure 4

Arsenite Bioremoval Efficiency of *Oceanobacillus picturae* Strain LW102 (a) Growth pattern of *Oceanobacillus picturae* strain LW102 in the absence and presence of different arsenite concentrations; (b) Reduction of arsenite concentration by *O. picturae* strain LW102 after 48 hours in SW7.5% medium supplemented with 1 ± 0.02 mM arsenite, resulting in a final concentration of 0.25 ± 0.07 mM; and (c) Percentage reduction of arsenite concentration achieved by *O. picturae*strain LW102 after 48 hours, demonstrating an approximate reduction of 80%. Error bars represent standard deviation (SD) of triplicate measurements (n = 3)

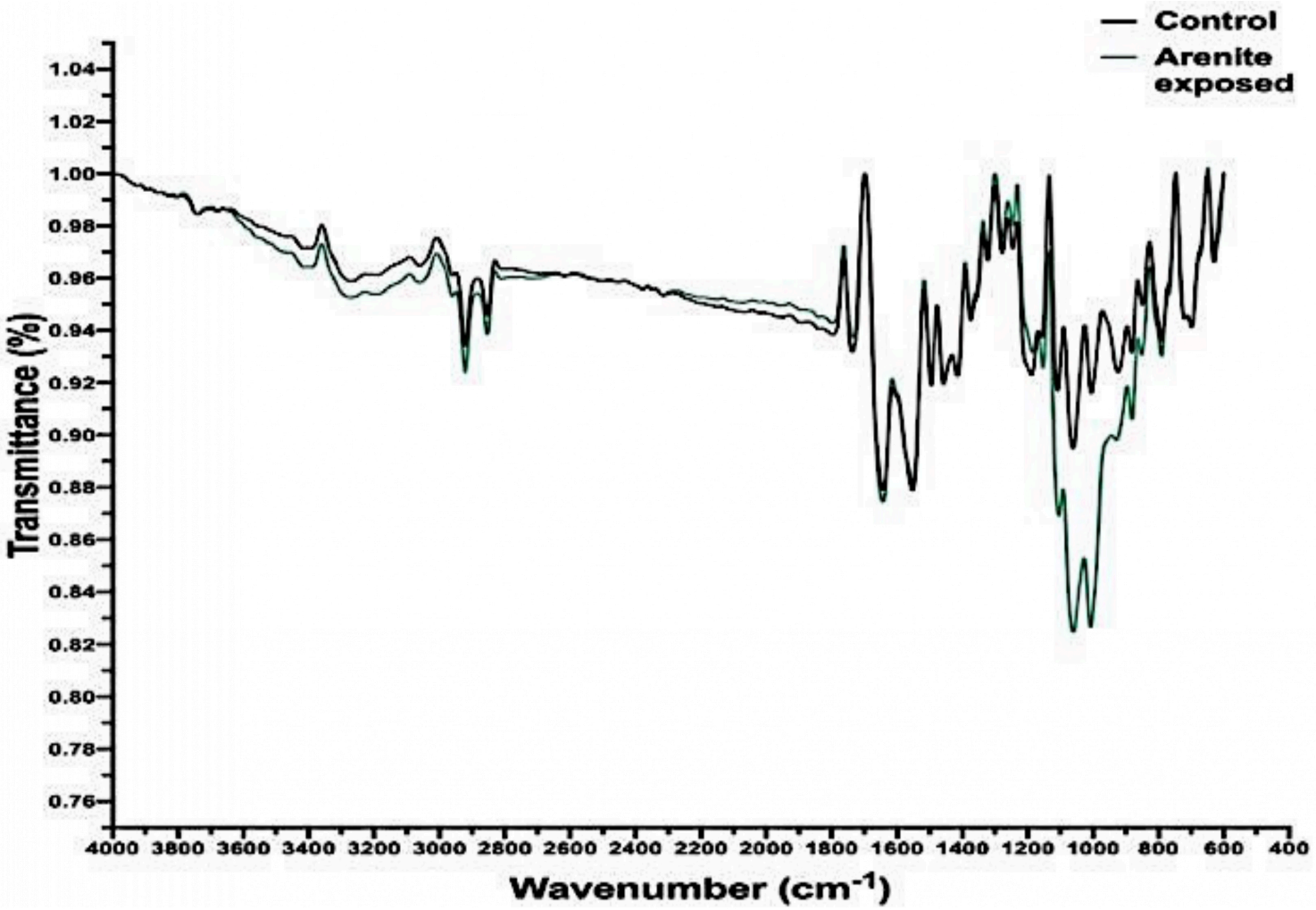

Figure 5

FTIR spectrum of *Oceanobacillus picturae* strain LW102. Green- Bacterial cells exposed to 1 mM arsenite, Black- Bacterial cells in the absence of arsenite

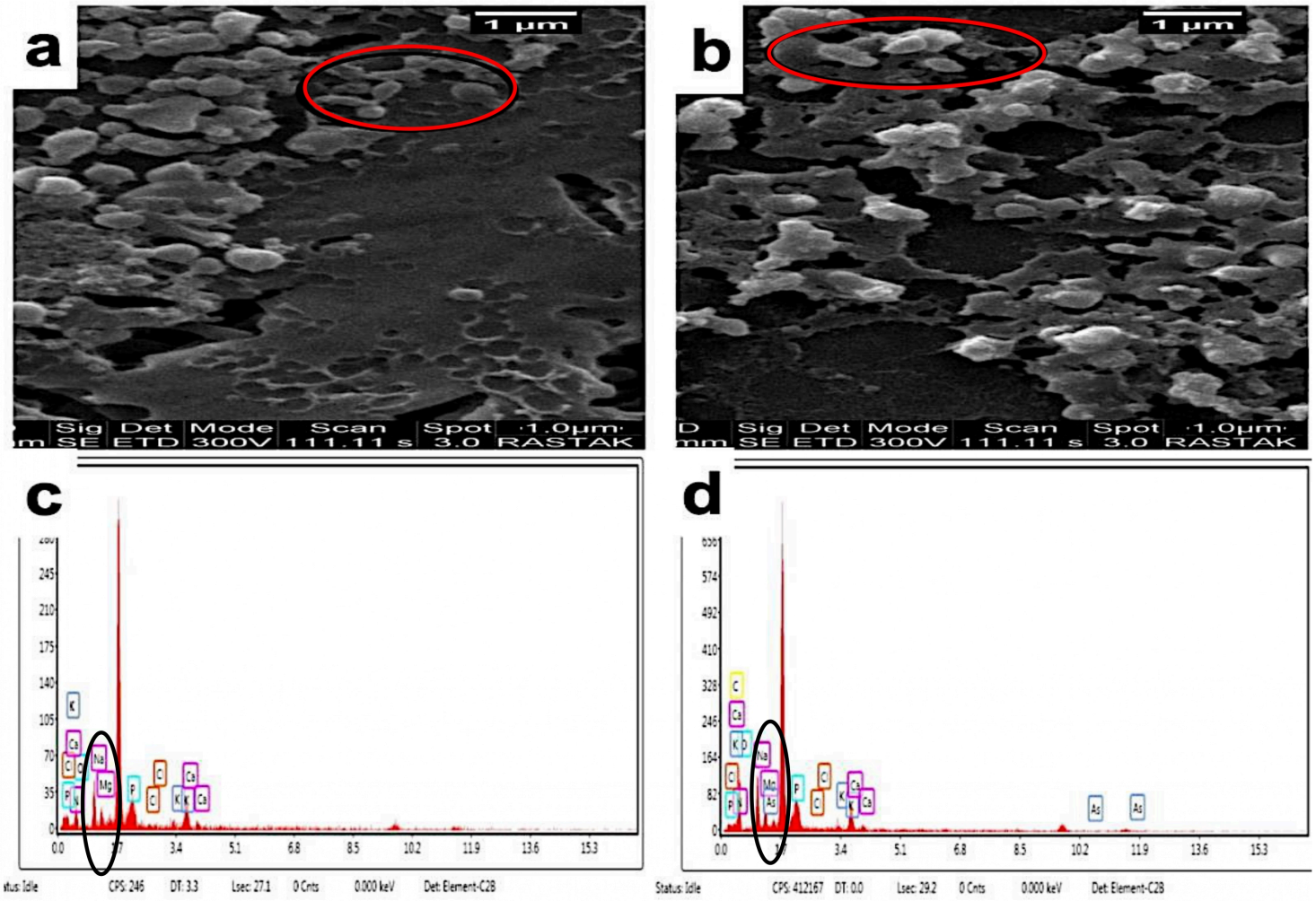

Figure 6

SEM-EDS micrograph of *Oceanobacillus picturae* strain LW102. (a) Bacterial cells in the absence of arsenite, (b) Bacterial cells exposed to 2 mM arsenite, with red circles highlighting differences between groups (c) EDS micrograph of bacterial cells without arsenite, (d) EDS micrograph of bacterial cells exposed to 2 mM arsenite, with black circles indicating distinct arsenic peaks

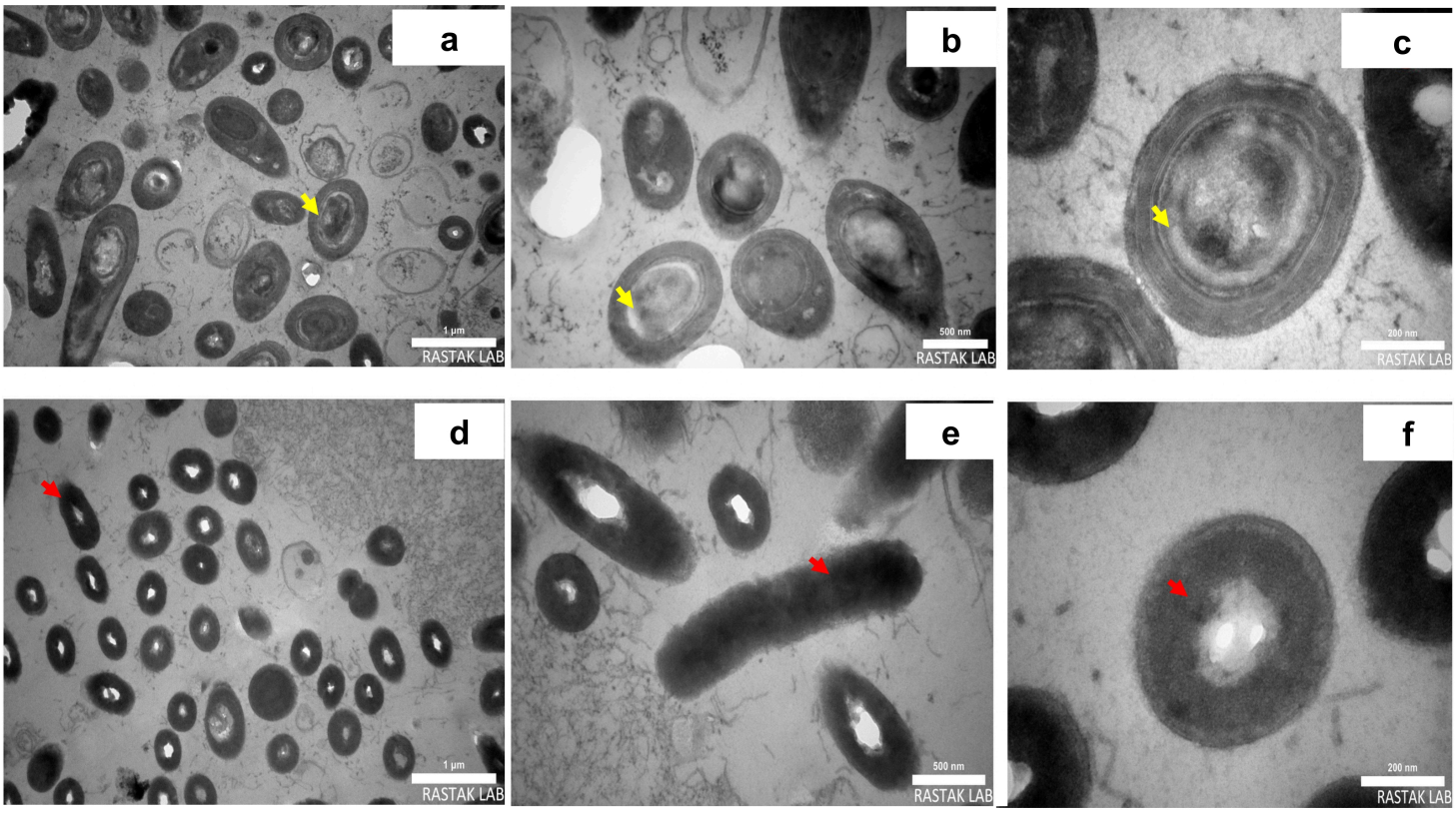

Figure 7

TEM micrograph of *Oceanobacillus picturae* strain LW102. (a, b, c) Bacterial cells in the absence of arsenite, (d, e, f) Bacteria cells exposed to 2 mM arsenite. Red arrows indicate regions of condensed cytoplasm associated with arsenite exposure, while yellow arrows highlight areas of clear cytoplasm. Scale bars are as follows: (a, d) = 1 micrometer; (b, e) = 500 nanometers; (c, f) = 200 nanometers

Supplementary Files

This is a list of supplementary files associated with this preprint. Click to download.

- Supplementary.docx